Discrete Rotational Energy for Polyatomic Molecules in Direct Simulation Monte Carlo

D. S. Liechty[1], D. Crouse[2] and T. E. Schwartzentruber[2][0000-0001-9064-2346]

[1] NASA Langley Research Center, Aerothermodynamics Branch, Hampton VA 23681, USA
[2] The University of Minnesota, Minneapolis MN 55455, USA

Abstract. Accurate prediction of aerothermodynamic loads in thermal non-equilibrium flows requires precise modeling of internal energy exchange. While previous direct simulation Monte Carlo frameworks have successfully implemented discrete rotational energy models for diatomic species, the treatment of polyatomic molecules has traditionally relied on continuous energy assumptions that break down at low temperatures and neglect critical high-temperature corrections. This study extends the discrete rotational energy models of Boyd and Gimelshein to fully encompass polyatomic molecules. The proposed framework implements quantized rotational energy level sampling for linear, spherical, and symmetric/asymmetric top rotors. Crucially, the model incorporates centrifugal distortion to address the limitations of the rigid-rotor assumption at hypersonic temperatures, and accounts for nuclear spin parity, which dictates the permissible rotational states and macroscopic specific heats at low temperatures. The model is verified through equilibrium sampling procedures, demonstrating agreement with theoretical quantum Boltzmann distributions and accurately reproducing thermophysical properties across a wide range of temperatures.

Keywords: DSMC, Discrete Rotation, Polyatomic.

1 Introduction

The environments experienced by vehicles upon entry into planetary atmospheres generally result in severe aerothermodynamic loading. These flows are characterized by the formation of strong shock waves, behind which high temperatures and non-equilibrium environments are generated, and the accurate prediction of internal energy relaxation processes (rotation, vibration, and electronic) and chemical kinetics become important.

In gas dynamics, the Boltzmann equation describes the rate of change, with respect to position and time, of the distribution function [1]. This relation is valid for gas flows across both the free molecular and continuum regimes. However, it is, in general, expensive and difficult to solve, so simplifications and assumptions are made. The continuum assumption leads to the Navier-Stokes equations of compressible gas dynamics, which is what computational fluid dynamics (CFD) solvers are based on. When the assumption of continuum flow breaks down, the de facto method of simulating rarefied

non-equilibrium flows has become the direct simulation Monte Carlo (DSMC) method [2,3].

Although consideration of all the internal processes mentioned above is required for the accurate prediction of the aerothermodynamic loads, this study focuses on the internal relaxation of the rotational energy of polyatomic molecules. Previous work [4] has described the implementation of a discrete rotational energy model for diatomic molecules. Prior to this, it was only possible to model rotational energy exchange between molecules in a continuous form using approaches such as, most famously, that of Borgnakke and Larsen (BL) [5]. The work of Boyd [4] followed the proposal of models which included the quantized nature of vibrational energy [6,7], leveraging the extension of the BL method to quantized internal energy modes. Later, Gimelshein et al. [8] extended this model to include polyatomic molecular energies. However, their work did not incorporate centrifugal distortion. In addition, no discussion was made with regards to spin parity, which is critical to account for at low temperatures. These additions are important for accurate aerothermodynamic modeling, as spin parity governs the macroscopic specific heats at the low temperatures of the free stream and wake, while centrifugal distortion corrects rigid-rotor inaccuracies at the high temperatures of the shock layer.

The purpose of the present study is to extend the discrete rotational energy models of Boyd [4] and Gimelshein et al. [8] for polyatomic molecules. Specifically, this work incorporates centrifugal distortion for high temperature accuracy and demonstrates the critical thermodynamic impact of nuclear spin isomers at low temperatures.

2 Rotation of Polyatomic Molecules

Molecules can be classified into different types of rotors depending on the relation between the three diagonal components of the moment of inertia, which define the rotational constants, A, B, and C. The types of rotors are then defined as: spherical top ($A = B = C$), oblate top ($A = B > C$), prolate top ($A > B = C$), linear ($A = 0, B = C$), and asymmetric top ($A \neq B \neq C$). Gimelshein et al. [8] detailed the energy and degeneracy definitions for the various types of polyatomic rotors, assuming a high-temperature continuous limit. Table 1 adapts these fundamental rigid-rotor definitions to account for the appropriate correction terms for centrifugal distortion. Note that for the purposes of this model, asymmetric rotors are approximated as nearly-prolate symmetric tops. The standard rigid-rotor approximation assumes that interatomic distances remain constant during rotation. Molecular bonds possess finite stiffness; consequently, the rotational motion of a molecule induces centrifugal forces that stretch these bonds. This increases the effective moment of inertia and, since rotational energy is inversely proportional to the moment of inertia, compresses the energy spacing at high rotational states, lowering the energy levels relative to standard rigid-rotor predictions.

To complicate matters further, at low temperatures deference must be given to spin parity (or nuclear spin statistics) which arises from the quantum mechanical requirement that the total wavefunction of a molecule must obey the Pauli exclusion principal when identical nuclei are exchanged. Depending on whether the identical nuclei are

Table 1. The different types of rotors and parameters required for sampling.

Type	$\epsilon^r_{J,K}/hc$	g_J
Spherical	$BJ(J+1) - D_J[J(J+1)]^2$	$(2J+1)^2$
Oblate	$BJ(J+1) + (C-B)K^2 - D_J[J(J+1)]^2 - D_{JK}J(J+1)K^2 - D_K K^4$	$\begin{cases} 2J+1 & if\ K=0 \\ 2(2J+1) & if\ K>0 \end{cases}$
Prolate	$BJ(J+1) + (A-B)K^2 - D_J[J(J+1)]^2 - D_{JK}J(J+1)K^2 - D_K K^4$	$\begin{cases} 2J+1 & if\ K=0 \\ 2(2J+1) & if\ K>0 \end{cases}$
Linear	$BJ(J+1) - D_J[J(J+1)]^2$	$2J+1$
Asym-metric	$BJ(J+1) + \left(A - \left(\frac{B+C}{2}\right)\right)K^2 - D_J[J(J+1)]^2 - D_{JK}J(J+1)K^2 - D_K K^4$	$\begin{cases} 2J+1 & if\ K=0 \\ 2(2J+1) & if\ K>0 \end{cases}$

fermions (half-integer spin) or bosons (integer spin), the total wavefunction must be respectively antisymmetric (changes sign) or symmetric (maintains sign) upon exchange. Because the total wavefunction is a product of the electronic, vibrational, rotational, and nuclear spin wavefunctions, the symmetry of the nuclear spin state directly dictates which rotational states are allowed. This leads into distinct "types" or isomers of the molecule that do not readily interconvert. This, in turn, modifies the degeneracy of each (J,K) rotational state and must be considered when computing the degeneracy and partition functions. The computation of the resulting modified degeneracies must be included when considering low temperature flows, but is beyond the scope of this study.

3 Modeling Polyatomic Discrete Rotational Energy in DSMC

To implement a discrete rotational energy model for polyatomic molecules, several sampling procedures must be established. First, quantized energy levels must be assigned via statistical sampling when a particle is introduced into the simulation at a prescribed temperature or when it undergoes diffuse reflection at a boundary. Second, rotational energy must be reassigned following inelastic intermolecular collisions. While post-collision assignment requires sampling from a joint translational-rotational distribution function, the underlying logic parallels the equilibrium sampling procedure. For brevity, this study focuses strictly on the equilibrium sampling framework.

Under equilibrium conditions, the distribution of the discrete rotational levels at a specified macroscopic temperature T follows the Boltzmann form

$$f_{J,K} = \frac{N_{J,K}}{N} = \frac{g_J e^{-\frac{\varepsilon_{J,K}}{kT}}}{\sum_j^{jmax} \sum_k^j g_J e^{-\frac{\varepsilon_{J,K}}{kT}}} = \frac{g_J e^{-\frac{\varepsilon_{J,K}}{kT}}}{Q_{J,K}} \tag{1}$$

Where k is the Boltzmann constant and Q is the partition function. Because the discrete quantum numbers cannot be sampled directly from this distribution via inversion, an acceptance-rejection scheme is employed. This scheme involves selecting the quantum number(s) from the normalized probability distribution

$$f' = \frac{f}{f_{max}} = \frac{g_J e^{-\frac{\varepsilon_{J,K}}{kT}}}{g_{J_s} e^{-\frac{\varepsilon_{J_s,K_s}}{kT}}} \tag{2}$$

where f_{max} is the normalization factor, and (J_s, K_s) represents the rotational quantum state at which Eq. (1) is maximized.

Previous works by Boyd [4] and Gimelshein et al. [8] detailed analytical methods to determine the optimal J_s that maximizes Eq. (1) for rigid rotors. However, the inclusion of centrifugal distortion introduces non-linearities that preclude a simple analytical maximum, requiring a numerical scan over the two-dimensional (J, K) parameter space. To ensure computational efficiency during this scan and the subsequent rejection sampling, strict physical and numerical bounds are enforced on the allowable quantum states. First, to optimize memory allocation, the quantum number K is evaluated strictly from 0 to J, with the symmetric $\pm K$ branches accounted for implicitly within the degeneracy function. Second, energy levels that become non-physical – such as those that invert and decrease past the centrifugal peak, or those that drop below zero – are truncated. Finally, high-energy states where the numerator of Eq. (1) falls below numerical significance (e.g., less than 1.0e-20) are omitted, effectively bounding the distribution at the dissociation limit.

4 Results and Discussion

To verify the derivation and implementation of the proposed discrete rotational energy framework, a series of zero-dimensional adiabatic reservoir simulations were conducted. To validate the model across all fundamental rotor types, a diverse set of polyatomic species was selected. The selected species, along with their associated spectroscopic constants and Variable Soft Sphere [9] (VSS) collision parameters, are summarized in Tables 2 and 3, respectively.

Table 2. Spectroscopy constants for various rotor types of species in their ground electronic states.

Species	Type	ζ_r	σ	A (cm^{-1})	B (cm^{-1})	C (cm^{-1})	D_J (cm^{-1})	D_{JK} (cm^{-1})	D_K (cm^{-1})
CH_4	Spherical	3	12	5.2412	5.2412	5.2412	1.1e-4	-	-
CH_3	Oblate	3	6	9.5779	9.5779	4.7428	1.1e-4	-2.3e-4	1.5e-4
CH_3^+	Prolate	3	6	9.3744	4.6114	4.6114	1.5e-4	-3.2e-4	2.1e-4
CO_2	Linear	2	2	0.0000	0.3915	0.0000	1.33e-7	-	-
CH_2	Asymmetric	3	2	73.8106	8.4504	7.1843	3.0e-3	4.0e-2	1.5

Table 3. VSS constants for various rotor types of species.

Species	Type	MW(amu)	d_{ref}(m)	T_{ref} (K)	ω	α
CH_4	Spherical	16.0425	4.292e-10	273.0	0.688	1.419
CH_3	Oblate	15.0345	4.267e-10	273.0	0.684	1.418
CH_3^+	Prolate	15.034	4.267e-10	273.0	0.684	1.418
CO_2	Linear	44.0095	4.147e-10	273.0	0.632	1.259
CH_2	Asymmetric	14.0266	4.267e-10	273.0	0.684	1.418

4.1 Definition of Rotational Temperature

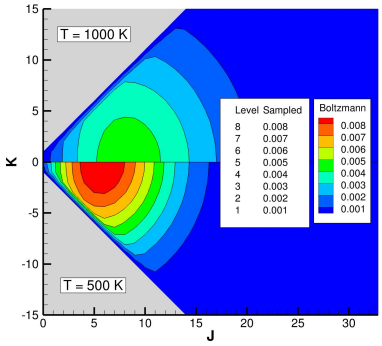

Fig. 1. Rotational level distribution for CH_3^+.

The methodology used to compute the macroscopic temperature from the sampled partition function is critical, particularly when the characteristic rotational temperature (Θ_r) is a significant fraction of the equilibrium temperature. In the classical limit ($\Theta_r/T \ll 1$), the discrete summation in the partition function is traditionally approximated as an integral [1]. However, as Boyd [3] demonstrated, consistency between the energy model and the macroscopic property evaluation is important; relying on the integral approximation yields incorrect temperatures in the low-temperature quantum regime and high-temperature effects of centrifugal distortion.

To strictly preserve thermodynamic consistency, the iterative methodology outlined by Civrais [10] is employed. This approach applies a truncated first-order Taylor expansion, specifically a Newton-Raphson scheme, to invert the discrete expected energy relation. Specifically, the objective function $f(T_r)$ is constructed using the theoretical mean rotational energy

$$E_r(T_r) = \frac{\sum_J^{Jmax} \sum_K^J \varepsilon_{J,K} g_J e^{-\frac{\varepsilon_{J,K}}{kT}}}{\sum_J^{Jmax} \sum_K^J g_J e^{-\frac{\varepsilon_{J,K}}{kT}}} \tag{3}$$

and the macroscopic rotational energy sampled from the DSMC algorithm, E_r^{DSMC}

$$f(T_r) = E_r^{DSMC} - E_r(T_r) \tag{4}$$

Setting $f(T_r) = 0$ allows for the iterative recovery of the true macroscopic rotational temperature. This iterative approach is highly robust and remains mathematically valid for both rigid-rotor models and those incorporating centrifugal distortion and spin isomers.

4.2 Equilibrium Distribution of Rotational Energy Levels

To verify the equilibrium sampling process outlined in Section 3, sampled distributions of generated particles are compared to the Boltzmann distribution for the prolate rotator in Fig. 1 where only one species is presented for brevity. A two-dimensional distribution is generated across the J/K energy level space where $K \in -J \leq K \leq J$. The distributions for CH_3^+ are presented in Fig. 1 at two temperatures. For each species/temperature, good agreement is observed between the distributions.

4.3 Thermophysical Properties

In addition to verifying the correct equilibrium temperature and distribution of energy states are reproducible, it is also important to demonstrate that thermophysical properties, such as the specific heat capacity, c_v, and enthalpy, h, are reproducible. From statistical mechanics [1], we know that

$$c_v = \left(\frac{\partial e}{\partial T}\right)_V \tag{5}$$

$$e = h = RT^2 \frac{\partial}{\partial T}[ln(Q)] \tag{6}$$

where the partition function is defined in Eq. (1). The expected energy and squared energy are defined as

$$\langle E \rangle = \frac{1}{Q}\sum_{J=0}^{\infty}\sum_{K=0}^{J} g_J e^{-\frac{\varepsilon_{J,K}}{kT}} \tag{7}$$

$$\langle E^2 \rangle = \frac{1}{Q}\sum_{J=0}^{\infty}\sum_{K=0}^{J} E^2 g_J e^{-\frac{\varepsilon_{J,K}}{kT}} \tag{8}$$

The specific heat and enthalpy can then be written as, summing over the isomers,

$$\frac{c_v}{R} = \sum_i X_i \frac{\langle E^2\rangle_i - \langle E\rangle_i^2}{(kT)^2} \tag{9}$$

$$\frac{h}{RT} = \sum_i X_i \frac{\langle E\rangle_i}{kT} \tag{10}$$

where X_i is the mole fraction of the isomer. This equation is equally valid for the sampled quantities.

The expected and sampled macroscopic properties are presented in Table 4. Under a classical, continuous assumption, the nondimensional specific heat (c_v/R) and enthalpy (h/RT) remain strictly constant: 1.0 for linear rotors and 1.5 for non-linear rotors. However, the discrete quantum model successfully captures several critical, physically accurate departures from this classical limit. First, the model naturally resolves nuclear spin isomer effects at low temperatures. For CO_2, because the I=0 spin parity halves the accessible states without shifting the ground state, the molecule behaves as a classical linear rotor ($c_v/R \approx 1$) even at 50 K. Conversely, the highly asymmetric CH_2 is subject to Pauli exclusion restrictions that forbid its absolute ground state, locking the ortho-isomer into an elevated K=1 state. The model captures this frozen-axis behavior, reflected by a linear specific heat combined with a significant zero-point energy offset in the enthalpy at 50 K, which subsequently "thaws" into a 3D rotor overshoot (Schottky anomaly) as temperature increases.

Table 4. Listing of theoretical, expected, and sampled non-dimensional specific heats.

Species	T^{eq} (K)	T^{samp}(K)	c_v^{exp}/R	c_v^{samp}/R	h^{exp}/RT	h^{samp}/RT
CH_4	50.0	50.0	1.56550	1.56575	1.41672	1.41685
	100.0	100.0	1.51264	1.51533	1.48099	1.48134
	500.0	499.9	1.51118	1.51014	1.50185	1.50151
	1000.0	1000.4	1.52300	1.52268	1.50944	1.51011
	3000.0	2999.5	1.57831	1.57758	1.53611	1.53582
	6000.0	6000.1	1.68387	1.68322	1.58346	1.58348
CH_3	50.0	50.0	1.51843	1.51858	1.45027	1.45037
	100.0	100.0	1.50088	1.50044	1.47710	1.47699
	500.0	500.2	1.50232	1.50395	1.49659	1.49709
	1000.0	1000.3	1.50463	1.50540	1.50003	1.50041
	3000.0	2999.6	1.51424	1.51517	1.50627	1.50607
	6000.0	5999.9	1.52962	1.52959	1.51405	1.51402
CH_3^+	50.0	50.0	1.51721	1.51658	1.45115	1.45053
	100.0	100.0	1.50102	1.50083	1.47746	1.47739
	500.0	499.9	1.50320	1.50249	1.49708	1.49665
	1000.0	1000.0	1.50643	1.50621	1.50095	1.50099
	3000.0	2998.4	1.51999	1.52086	1.50907	1.50828
	6000.0	5999.8	1.54235	1.54218	1.52001	1.51995
CO_2	50.0	50.0	1.00013	1.00046	0.99633	0.99609
	100.0	100.0	1.00025	1.00195	0.99826	0.99871
	500.0	499.9	1.00123	1.00223	1.00024	1.00011
	1000.0	1000.2	1.00247	1.00263	1.00104	1.00125
	3000.0	3000.6	1.00752	1.00785	1.00367	1.00387
	6000.0	6000.9	1.01555	1.01376	1.00759	1.00774
CH_2	50.0	50.0	1.00650	1.00596	2.50405	2.50413
	100.0	100.0	1.19979	1.19903	1.79854	1.79854
	500.0	499.9	1.64153	1.64015	1.59797	1.59751
	1000.0	999.7	1.60082	1.60045	1.61540	1.61500
	3000.0	2994.5	1.47782	1.47902	1.54483	1.54211
	6000.0	5992.2	1.48689	1.49005	1.51319	1.51125

Second, as temperatures elevate, the model successfully captures the onset of centrifugal distortion, which drives a strict increase in the specific heat as molecular bonds stretch. However, at extreme temperatures, the specific heat begins to roll off, dropping below the classical limits. The model correctly predicts this physical decrease, which is a direct thermodynamic consequence of rotational energy level truncation at the dissociation limit and the saturation of available high-energy quantum states.

5 Conclusions

A discrete rotational energy model for polyatomic molecules has been successfully implemented and verified within the direct simulation Monte Carly framework. By treating rotational energy as quantized levels governed by specific selection rules – rather than relying on the traditional continuous energy assumption – the current approach provides a strictly physically accurate representation of internal energy states. This distinction is important for low-temperature flows, where quantum effects such as the

"freezing out" of rotational axes and nuclear spin parity restrictions significantly alter the specific heat and bulk thermodynamic properties of the gas.

The model was subjected to several verification cases, yielding the following outcomes:

1) The equilibrium sampling procedures successfully reproduce theoretical Boltzmann distributions for a diverse set of species, correctly distinguishing between linear, spherical and symmetric/asymmetric top rotors.
2) The sampled specific heats and enthalpies demonstrate good agreement with theoretical values. The model accurately captures low-temperature Schottky anomalies (specific heat overshoot) and zero-point energy offsets driven by spin isomers – phenomena entirely missed by continuous energy formulations.
3) To address the limitations of the rigid-rotor assumption at elevated temperatures, a framework for centrifugal distortion was integrated into the discrete model. The model was able to account for non-rigid bond stretching at high rotational energies, predicting the correct elevation of the rotational specific heat capacity.

Overall, the discrete rotational model systematically overcomes the limitations of the continuous energy assumption at low temperatures. The integration of centrifugal distortion represents a significant step toward resolving rigid-rotor inaccuracies at high temperatures.

References

1. Vincenti, W.G, Kruger, C.H.: Introduction to Physical Gas Dynamics. 2nd edn. Wiley, New York (1965)
2. Bird, G.A.: Molecular Gas Dynamics and the Direct Simulation of Gas Flows. 2nd edn. Oxford University Press, Inc., New York (1994)
3. Boyd, I.D., Schwartzentruber, T.E.: Nonequilibrium Gas Dynamics and Molecular Simulation. Cambridge University Press, New York (2017)
4. Boyd, I.D.: Relaxation of discrete rotational energy distributions using a Monte Carlo method. Physics of Fluids A **5**(9), 2278-2286 (1993)
5. Borgnakke, C., Larsen, P.S.: Statistical collision model for Monte Carlo simulation of polyatomic gas mixtures. Journal of Computational Physics **18**, 405-420 (1975)
6. Haas, B.L.: Models of energy-exchange mechanics applicable to a particle simulation of reactive flow. Journal of Thermophysics **6**(2), 200-207 (1992)
7. Gimelshein, S.F., Boyd, I.D., Ivanov, M.S.: Modeling of Internal Energy Transfer in Plume Flows of Polyatomic Molecules by the DSMC Method. AIAA Pap. No 99-0738 (1999)
8. Bergemann, F., Boyd, I.D.: New discrete vibrational energy model for the direct simulation Monte Carlo method. Progress in Astronautics and Aeronautics **158**, 174-183 (1994)
9. Koura, K., Matsumoto, H.: Variable soft sphere molecular model for inverse-power-law or Lennard-Jones potential. Physics of Fluids A **3**(10), 2459-2465 (1991)
10. Civrais, C.H.B., White, C., Steijl, R.: Vibrational modeling with an anharmonic oscillator model in direct simulation Monte Carlo. Journal of Thermophysics and Heat Transfer **37**(3) 534-548 (2023)